



Cell cycle arrest and induction of apoptosis of newly synthesized pyranoquinoline derivatives under microwave irradiation

Ahmed M. Fouda¹ · Ayman M. S. Youssef^{1,2} · Tarek H. Affi³ · Ahmed Mora⁴ · Ahmed M. El-Agrody⁴

Received: 22 January 2019 / Accepted: 8 March 2019
© Springer Science+Business Media, LLC, part of Springer Nature 2019

Abstract

A set of 2-amino-4-aryl-4*H*-pyrano[3,2-*h*]quinoline-3-carbonitrile derivatives were prepared via a one-pot, three-component condensation reaction between the substituted hydroxyquinoline derivatives, some aryl and/or hetaryl aldehydes, and malononitrile in an ethanol/piperidine solution in a microwave irradiation environment. The structure of the prepared compounds was instituted on the foundations of their spectral data: IR, ¹H NMR, ¹³C NMR, and MS. Four human cancer cell lines, MCF-7, HCT-116, HepG-2, and A549 were utilized to evaluate the antiproliferative properties of the target compounds in comparison to the positive controls, Vinblastine and Colchicine using the MTT viability assay. The cell cycle arrest behavior, detected by propidium iodide as well as the apoptosis induction, which was monitored by the flow cytometer, using the Annexin V-FITC kits, was investigated. The results illustrated that the potent cytotoxic compounds induce cell cycle arrest at the G2/M phases and trigger apoptosis in the different tested cancer cells. Finally, the structure–activity relationship (SAR) study showcases the substitution of some specific groups at the 4-, 6-, and 9-positions in the prepared 2-amino-4*H*-pyrano[3,2-*h*]quinoline derivatives, which indicates that the lipophilicity manipulates the ability of these moieties against the diverse cell lines.

Keywords Microwave synthesis · 4*H*-Pyrano[3,2-*h*]quinoline · Antitumor · Cell cycle · SAR

Introduction

A heterocyclic-based quinoline nucleus is prevalent in naturally occurring quinoline alkaloids, which are therapeutics and synthetic analogs with significant biological activities, such as antimicrobial (Prasad et al. 2017; Hassanin et al. 2012; Chang et al. 2010; Thomas et al. 2010),

antitubercular (Balamurugan et al. 2010), antiasthmatic (Doube et al. 1998), antimalarial (Kaur et al. 2009; Sparatore et al. 2008), antidiabetic (Edmont et al. 2000), anti-breast cancer (Shi et al. 2008), immunosuppressive (Batt et al. 1998), antiviral (Narsinh and Anamik 2001), HIV-1 integrase inhibitory (Sechi et al. 2009), and antiproliferative (Mol et al. 1984) activities. The fused pyranoquinoline moiety is an extremely common structural motif, existing in many naturally occurring or biologically active alkaloids, such as flindersine, atanine, tabouensinium chloride, zanthoxylum simulans, oricine, verprisine, and araliopsis tabouensis (Wabo et al. 2005; Chen et al. 1997, 1994; Ramesh et al. 1984). The unique biological activity of the pyranoquinoline derivatives has made these compounds as privileged targets in recent medicinal studies. For instance, compounds that contain a pyranoquinoline nucleus have been frequently used for bactericidal and bacteriolytic activities (Siliveri et al. 2017; Magesh et al. 2004), acetylcholinesterase inhibitor (Marco and Martinez-Grau 1997), antiallergenic (Kamperdick et al. 1999; et al. Cairns et al. 1985), anti-inflammatory (Chen et al. 2007), antimalarial (Isaka et al. 2001), calcium-signaling inhibition (Koizumi et al. 2007), platelet aggregation (Chen et al. 1997) and

Supplementary information The online version of this article (<https://doi.org/10.1007/s00044-019-02325-5>) contains supplementary material, which is available to authorised users.

✉ Ahmed M. Fouda
amfouda@hotmail.com

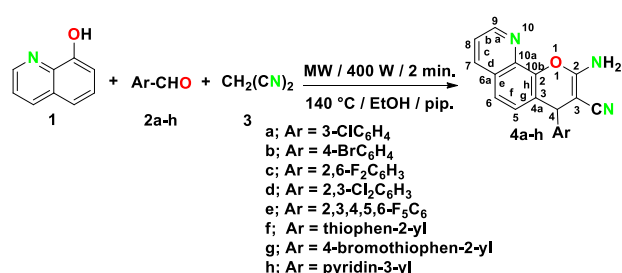
- ¹ Chemistry Department, Faculty of Science, King Khalid University, Abha 61413, Saudi Arabia
- ² Chemistry Department, Faculty of Science, Fayoum University, Fayoum, Egypt
- ³ Chemistry Department, Faculty of Science, Taibah University, Al-Madinah Al-Munawarah 30002, Saudi Arabia
- ⁴ Chemistry Department, Faculty of Science, Al-Azhar University, Nar City, Cairo 11884, Egypt

antitumor (Fouda 2017; Hammouda et al. 2015; Al-Ghamdi et al. 2012; El-Agrody et al. 2013; 2012) activities and agents. Recently, a pyranoquinoline nucleus has been employed in the pharmacophores with potential medicinal features against various diseases, like Alzheimer's (Maalej et al. 2012), venereal (Wabo et al. 2005) and psychotropic (Nesterova et al. 1995). Based on these outcomes, we have designed and synthesized a number of related 2-amino-4-aryl-4*H*-pyrano[3,2-*h*]quinoline-3-carbonitrile derivatives and assessed their pharmacological effects. The present study also examines the mechanisms underlying the cytotoxicity of the most potent compounds, utilizing cell cycle analyses, and the structure–activity relationships (SAR) of the desired molecules will be highlighted on the effect of the substituents at the 4-, 6-, and 9-positions towards the antitumor activity.

Results and discussion

Chemistry

Microwave heating is renowned for accelerating organic reactions, shortening the reaction time, producing high yields, having a solvent-free state, or being in ethanol (Mekheimer and Sadek 2009; Surpur et al. 2009; Wu and Larhed 2005; Kidwai et al. 2005; Kappe 2004; Shi et al. 2004), and aiding in generating products not attainable through the classical thermal methods (Fouda 2017; Hammouda et al. 2015; Al-Ghamdi et al. 2012; El-Agrody and Al-Ghamdi 2011), which require a prolonged reaction time, stoichiometric reagents, and toxic solvents and generate only moderate yields of the product. Our methodology, concerning the targeted heterocyclic-based pyranoquinoline compounds, was initiated through the synthesis of 2-amino-4-aryl-4*H*-pyrano[3,2-*h*]quinoline-3-carbonitrile derivatives (**4a–h**) via a one-pot, three-component condensation between the equimolar amounts of 8-hydroxyquinoline (**1**), various aryl or hetaryl aldehydes (**2a–h**), and malononitrile (**3**) in ethanol, catalyzed by piperidine under microwave



Scheme 1 2-Amino-4-aryl-4*H*-pyrano[3,2-*h*]quinoline-3-carbonitrile derivatives (**4a–h**)

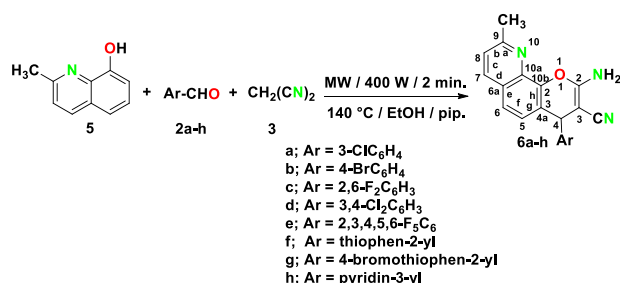
irradiation conditions for 2 min at 140 °C, presented in Scheme 1.

The assignment of the structures of the **4a–h** derivatives was established on the basis of their spectral data (IR, ¹H NMR, ¹³C NMR and MS) and elemental analyses. For example, the IR spectrum of compound **4c** showed absorption bands at ν 3481, 3330, and 3219 cm⁻¹ for NH₂ in addition to the absorption band of the cyano group at ν 2190 cm⁻¹. On the other hand, the ¹H NMR spectrum of **4c** revealed the presence of the NH₂ protons at δ 7.30 ppm with the presence of the aliphatic methine proton at δ 5.42 ppm. The ¹³C NMR spectrum of **4c** revealed that the carbon methine signal resonate at δ 30.56 ppm. Furthermore, the mass spectrum of **4c** exhibited (*m/z*) with a base peak at 335 (*M*⁺, 100).

In a similar approach, the reaction of 8-hydroxy-2-methylquinoline (**5**) with aryl or hetaryl aldehydes (**2a–h**) and malononitrile (**3**) in an ethanol/piperidine solution under microwave irradiation conditions yielded the 2-amino-4-aryl-9-methyl-4*H*-pyrano[3,2-*h*]quinoline-3-carbonitrile derivatives (**6a–h**), as disclosed in Scheme 2.

The spectroscopic data (IR, ¹H NMR, ¹³C NMR, and MS) and the elemental analyses of compounds **6a–h** were consistent with the predicted structure. The IR spectrum of derivative **6e** revealed that the NH₂ and cyano groups' absorption bands appeared at ν 3409, 3342, 3197 cm⁻¹, and 2208 cm⁻¹, respectively. Additionally, their ¹H NMR spectrum displayed three signals at δ 7.28, δ 5.9, and δ 2.71 ppm, due to the NH₂, CH, and CH₃ groups, respectively. The ¹³C NMR spectrum of **6e** displayed two signals, resonating at δ 31.03 and δ 23.43 ppm, which can be attributed to the CH (pyrano) and CH₃ carbons, respectively. Also, the mass spectrum showed (*m/z*), 403 (*M*⁺, 96.79) with a base peak at 40 (100).

Following the same methodology, the interaction of the 5-chloro-8-hydroxyquinoline (**7**) with several aryl or hetaryl aldehydes (**2a–i**) and malononitrile (**3**) in an ethanol/piperidine solution in a microwave irradiation environment delivered the 2-amino-4-aryl-6-chloro-4*H*-pyrano[3,2-*h*]quinoline-3-carbonitrile derivatives (**8a–i**), Scheme 3. The newly formed products **8a–i** were characterized by their IR,



Scheme 2 2-Amino-4-aryl-9-methyl-4*H*-pyrano[3,2-*h*]quinoline-3-carbonitrile derivatives (**6a–h**)

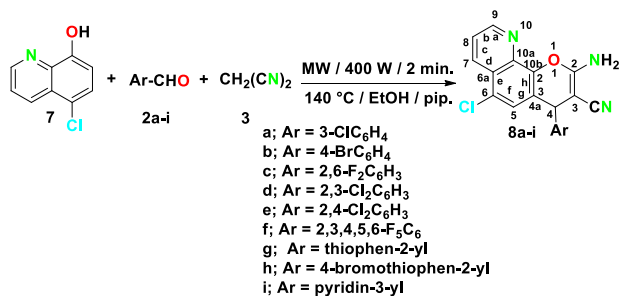
^1H , and ^{13}C NMR spectra. Supporting evidence for the suggested structures arises from the infrared absorption bands of compound **8g** at ν 3443, 3344, 3238 cm^{-1} , and 2213 cm^{-1} for the NH_2 and cyano groups. On the contrary, the ^1H NMR spectrum of **8g** revealed the presence of the NH_2 protons at δ 7.48 ppm and the aliphatic methine proton at δ 5.58 ppm. Further confirmation resulted from the ^{13}C NMR spectrum of **8g** that exhibited signal, resonating at δ 35.98 ppm for the CH carbon. Moreover, the mass spectrum of **8g** revealed (m/z), 341 ($\text{M}^+ + 2$, 32.08) with a base peak at 339 (M^+ , 100).

The maximum power of the microwave irradiation was optimized by repeating all the reactions at different watt powers and periods of times. The optimum condition was obtained by using microwave irradiations at 400 W and a reaction time of 2 min, which gave the highest yield of the desired compounds. It is also important to note that the 4-position of compounds **4a–h**, **6a–h**, and **8a–i** are chiral centers, and all the reactions were controlled, using the thin layer chromatography (TLC) technique.

Biological activity

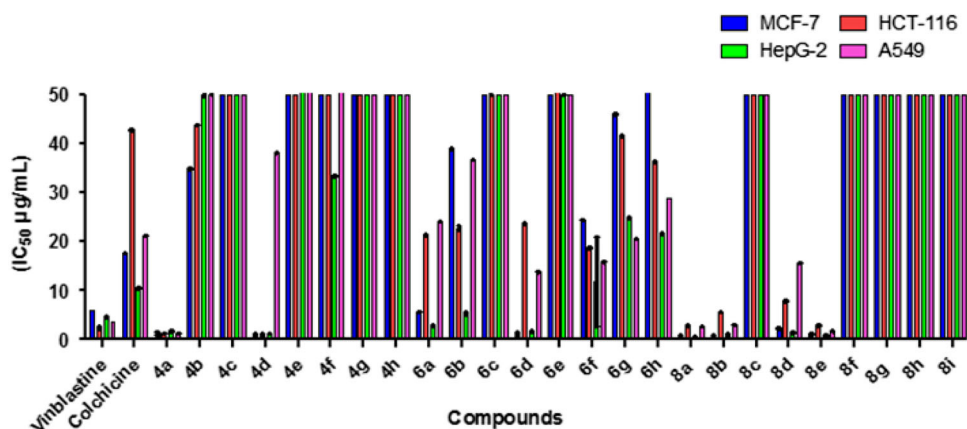
In vitro cytotoxic activity

The MTT assay (Demirci and Bas,er 2002; Rahman et al. 2001; Mosmann 1983) was performed to evaluate the



Scheme 3 2-Amino-4-aryl-6-chloro-4H-pyrano[3,2-h]quinoline-3-carbonitrile derivatives (**8a–i**)

Fig. 1 IC_{50} values expressed in ($\mu\text{g}/\text{ml}$) of 2-amino-4-aryl-4H-pyrano[3,2-h]quinoline-3-carbonitrile derivatives against MCF-7, HCT-116, HepG-2, and A549 tumor cells



cytotoxic effects of the 2-amino-4-aryl-4H-pyrano[3,2-h]quinoline-3-carbonitrile derivatives (**4**, **6**, **8**) against the selected human cancer cell lines, namely: mammary gland breast cancer (MCF-7), human colon cancer (HCT-116), human hepatocellular carcinoma (HepG-2), and lung carcinoma (A549), using Vinblastine and Colchicine as reference compounds. The in vitro cytotoxicity evaluation was achieved under various concentrations, ranging from 0 to 50 $\mu\text{g}/\text{ml}$. The results were expressed as growth inhibitory concentration (IC_{50}) values, where the necessitated concentration produced a 50% inhibition of cell growth after 24 h of incubation, compared to the untreated controls. The IC_{50} values are summarized in Fig. 1 and Table 1.

From the obtained results, it was elucidated that most of the prepared compounds displayed excellent to modest or weak growth inhibitory activity against the tested cancer cell lines. Investigations of the cytotoxic activity against MCF-7, HCT-116, HepG-2, and A549 tumor cell lines indicated that the MCF-7 was the most sensitive cell line to the influence of the new derivatives. Overall, compounds **4a**, **d** ($\text{IC}_{50} = 1.42 \pm 0.3$, 1.35 ± 0.2 , 1.87 ± 0.2 , 1.23 ± 0.1 and 1.17 ± 0.11 , 1.3 ± 0.12 , 1.41 ± 0.18 , $38 \pm 0.03 \mu\text{g}/\text{ml}$, respectively), **6a**, **d** ($\text{IC}_{50} = 5.79 \pm 0.01$, 3.01 ± 0.11 and 1.24 ± 0.3 , $1.83 \pm 0.2 \mu\text{g}/\text{ml}$) and **8a**, **b**, **d**, **e** ($\text{IC}_{50} = 0.9 \pm 0.07$, 3.04 ± 0.2 , 0.7 ± 0.06 , 2.67 ± 0.07 ; 0.99 ± 0.01 , 5.81 ± 0.11 , 1.23 ± 0.03 , 3.1 ± 0.01 ; 2.47 ± 0.13 , 7.94 ± 0.05 , 1.48 ± 0.11 , 15.6 ± 0.13 and 1.18 ± 0.14 , 3.01 ± 0.22 , 0.87 ± 0.12 , $1.79 \pm 0.14 \mu\text{g}/\text{ml}$, respectively) were found to be the most potent derivatives of all the tested compounds against the MCF-7, HCT-116, HepG-2, and A549 tumor cell lines. In general, the other compounds demonstrated moderate to fair cytotoxic activities against the four tumor cell types.

G2/M phase cell cycle arrest in treated cancer cells

In order to explain the effect of the most potent newly synthesized compounds (**4a**, **d**, **6d**, **8a**, **b**, **d**, **e**) against the different cancer cell lines, we have performed a cell cycle

Table 1 IC₅₀ of the target compounds against MCF-7, HCT-116, HepG-2, and A549 cell lines

Compound	Ar	IC ₅₀ (μg/ml) ^a			
		MCF-7	HCT-116	HepG-2	A549
4a	3-ClC ₆ H ₄	1.42 ± 0.3 ^b	1.35 ± 0.2 ^b	1.87 ± 0.2 ^b	1.23 ± 0.1 ^b
4b	4-BrC ₆ H ₄	34.8 ± 0.15 ^c	43.7 ± 0.13 ^c	NA ^c	w ^b
4c	2,6-F ₂ C ₆ H ₃	w	w	w	w
4d	2,3-Cl ₂ C ₆ H ₃	1.17 ± 0.11 ^b	1.3 ± 0.12 ^b	1.41 ± 0.18 ^b	38 ± 0.03 ^b
4e	2,3,4,5,6-F ₅ C ₆	w	w	w	w
4f	thiophen-2-yl	w	w	33.3 ± 0.02	52.5 ± 0.06
4g	4-bromothiophen-2-yl	w	w	w	w
4h	pyridin-3-yl	w	w	w	w
6a	3-ClC ₆ H ₄	5.79 ± 0.01 ^b	21.4 ± 0.1 ^b	3.01 ± 0.11 ^b	24 ± 0.01 ^b
6b	4-BrC ₆ H ₄	38.9 ± 0.14 ^c	22.8 ± 0.13 ^c	5.5 ± 0.13 ^c	36.7 ± 0.14 ^b
6c	2,6-F ₂ C ₆ H ₃	w	w	w	w
6d	3,4-Cl ₂ C ₆ H ₃	1.24 ± 0.3 ^b	23.7 ± 0.04 ^b	1.83 ± 0.2 ^b	13.7 ± 0.3 ^b
6e	2,3,4,5,6-F ₅ C ₆	w	w	w	w
6f	thiophen-2-yl	24.4 ± 0.1	18.8 ± 0.2	11.8 ± 0.3	15.5 ± 0.2
6g	4-bromothiophen-2-yl	45.9 ± 0.2	41.54 ± 0.14	24.8 ± 0.16	20.5 ± 0.3
6h	pyridin-3-yl	w	36.4 ± 0.13	21.7 ± 0.1	28.9 ± 0.06
8a	3-ClC ₆ H ₄	0.9 ± 0.07 ^b	3.04 ± 0.2 ^b	0.7 ± 0.06 ^b	2.67 ± 0.07
8b	4-BrC ₆ H ₄	0.99 ± 0.01 ^b	5.81 ± 0.11 ^b	1.23 ± 0.03 ^b	3.1 ± 0.01 ^b
8c	2,6-F ₂ C ₆ H ₃	w	w	w	w
8d	2,3-Cl ₂ C ₆ H ₃	2.47 ± 0.13 ^b	7.94 ± 0.05 ^b	1.48 ± 0.11 ^b	15.6 ± 0.13 ^b
8e	2,4-Cl ₂ C ₆ H ₃	1.18 ± 0.14 ^b	3.01 ± 0.22 ^b	0.87 ± 0.12 ^b	1.79 ± 0.14 ^b
8f	2,3,4,5,6-F ₅ C ₆	w	w	w	w
8g	thiophen-2-yl	w	w	w	w
8h	4-bromothiophen-2-yl	w	w	w	w
8i	pyridin-3-yl	w	w	w	w
Vinblastine	—	6.1 ± 0.01	2.6 ± 0.04	4.6 ± 0.11	3.78 ± 0.01
Colchicine	—	17.7 ± 0.03	42.8 ± 0.06	10.6 ± 0.13	21.3 ± 0.03

^aIC₅₀ values expressed in μg/ml as the mean values of triplicate wells from at least three experiments and are reported as the mean ± standard error
w = weak activity (IC₅₀ ≥ 50 μg/ml)

^bFouda 2017

^cEl-Agrody et al. 2013 and NA not active

analysis, using the flow cytometer (Qu et al. 2016; Shen et al. 2009). The cell cycle distribution for the untreated control cells, reference drugs, and compound **8b** is displayed in Fig. 2a, b as the percentage of cells containing 2n (G1 phase), 4n (G2 and M phases), and 4n > 3n > 2n of

DNA amount (S phase), assessed via PI staining. All the tested compounds expressed an increased cell number at the G2/M phases, up to 40% after 24 h, as compared to the 10% in the control cells, Fig. 2c. These results are accompanied by a 10% decrease in the cell number at the S phase and a

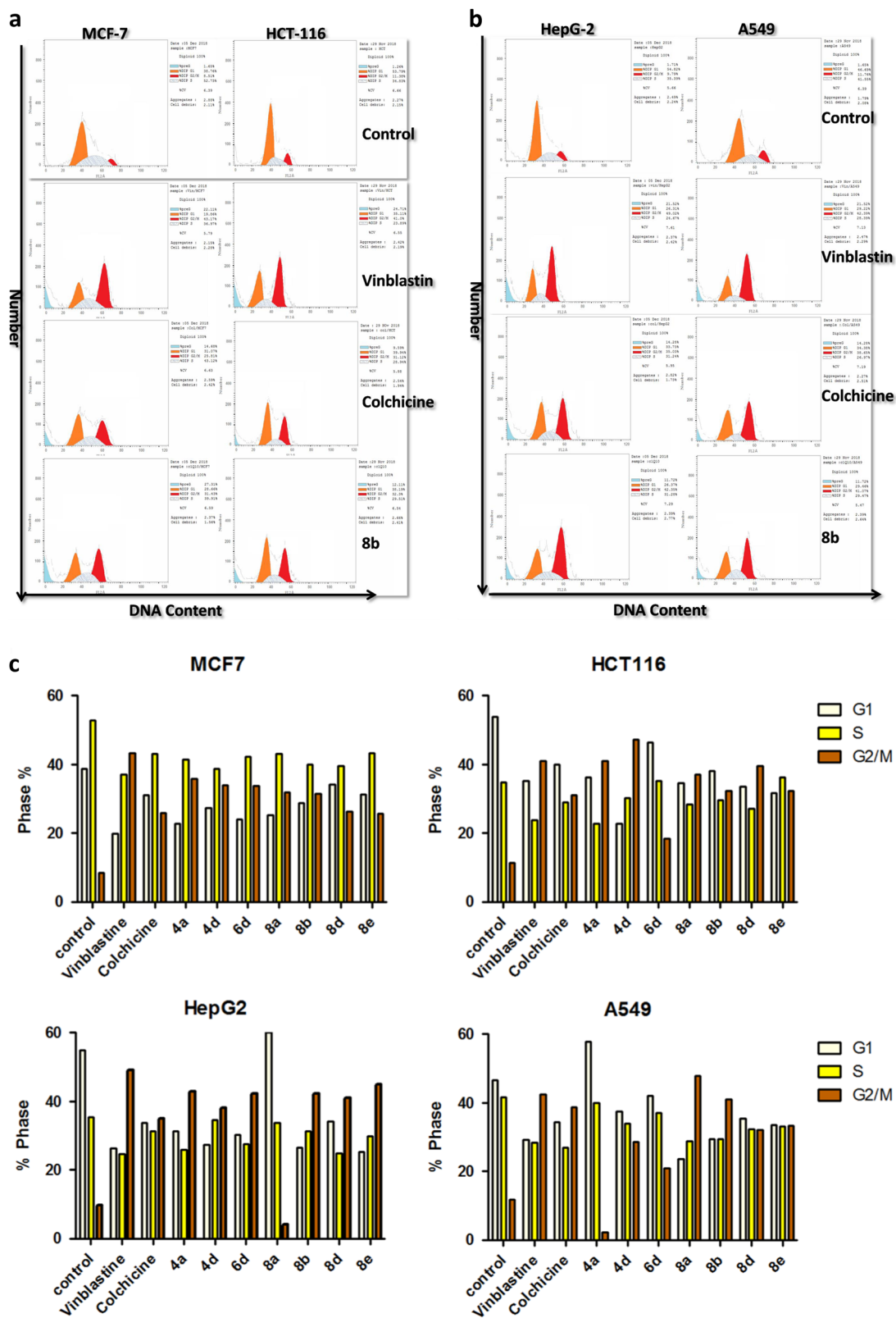


Fig. 2 a, b Representative histograms of DNA content distribution of cell cycle phases of MCF-7 and HCT-116 (a), HepG-2 and A549 (b) of untreated control cells, reference drugs and compound **8b**. DNA content was stained with P). Other compounds **4a, d, 6d** and **8a, d, e**

histograms results are shown in supplementary data Fig. 2d. **c** The graphical representation of the trend in cell cycle arrest of MCF-7, HCT-116, HepG-2, and A549 cells after treatment with IC₅₀ concentration of tested compounds for 24 h

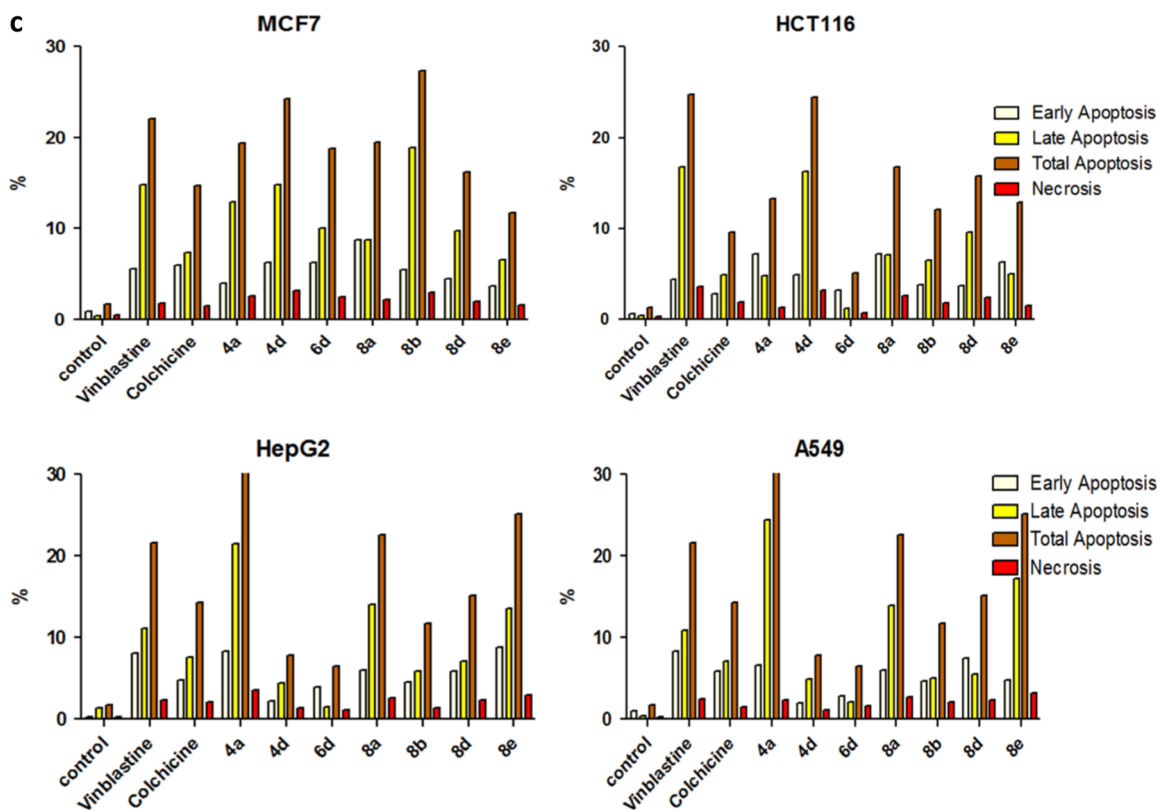
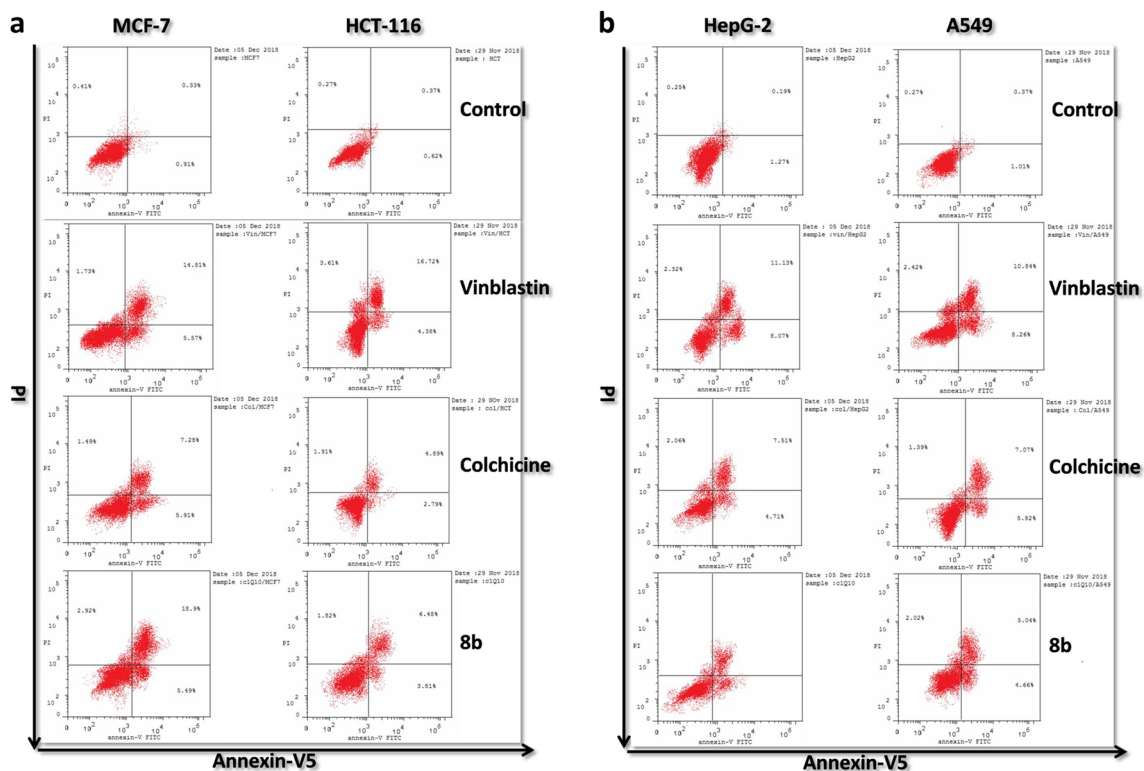


Fig. 3 a, b Annexin V/PI assay showing dot plots of MCF-7 and HCT-116 (a), HepG-2 and A549 (b) of untreated control cells, and treated cells with reference drugs and compound **8b**. Other compounds **4a, d, 6d** and **8a, d, e** dot plots results are shown in supplementary data Fig.

3d. c The percentage of different cell lines in different stages following the treatment with IC₅₀ concentration of tested compounds for 24 assessed via Annexin V/PI assay and flow cytometry

40% decrease in the G1 phase for all cell lines in comparison to the untreated control cells, Fig. 2b. Moreover, the tested compounds showed higher cell cycle arrest percentages at G2/M than the reference drug Colchicine while they showed almost the same result as Vinblastine. However, the compound **4a** in the case of the A549 cell line and compound **8a** in the case of HepG-2 have presented a slight increase in the G1 phase cell number and a decrease in the G2/M phases with no differences in the S phase when evaluated against the control cells.

Apoptosis induction in treated cancer cells

Many anticancer compounds exert their effect by blocking the cell cycle progression, inducing apoptosis, or the combined effect of both. To verify the linked relation of the cell cycle arrest and apoptosis, an Annexin/PI double staining assay was performed (Van Engeland et al. 1998; Vermes et al. 1995). Dot plots for the untreated control cells, reference drugs, and compound **8b** are shown in Fig. 3a, b.

The percentage of both the early (Annexin V positive, PI negative) and late (Annexin V positive, PI positive) apoptosis for the treated cells are shown in Fig. 3c. All cell lines treated with compounds **4a** and **8a, b, 8d, and 8e** for 24 h generated high apoptosis percentages more or less equal to Colchicine and Vinblastine. Furthermore, we notice that the MCF-7, HepG-2, and A549 cells entered a late apoptotic stage after their treatment with compound **4a**. However, compounds **4d** and **6d** displayed the lowest percentage of apoptosis in the case of HCT-116, HepG-2, and A549 cells. Necrotic cells were not observed with any of the tested compounds. The results corroborated that the induction of cytotoxicity occurs through the mechanisms associated with apoptosis.

SAR studies

The preliminary SAR study was centered on the effect of the replacement of the hydrogen atoms on the phenyl or hetero ring at the 4-position of the 4*H*-pyrano[3,2-*h*]quinoline scaffold by the different halogen atoms and the chloro or methyl group at the 6- and 9-positions. In a comparison of the cytotoxic activities of the three series **4a–h**, **6a–h**, and **8a–i** against the MCF-7, HCT-116, HepG-2, and A549 tumor cell types, we discovered that the introduction of this modification has decreased the IC₅₀ values of the first members (monosubstituent, **4a**, IC₅₀ = 1.42 ± 0.3, 1.35 ± 0.2, 1.87 ± 0.2, and 1.23 ± 0.1 µg/ml, respectively) and the second members (disubstituents **4d**, IC₅₀ = 1.17 ± 0.11, 1.3 ± 0.12, 1.41 ± 0.18, and 38 ± 0.03, respectively) and increased the IC₅₀ values (moderate to weak activities) for the third and fourth members (polysubstituents and hetero

group) against all the tumor cells as compared to the standard drugs Vinblastine and Colchicine (IC₅₀ = 6.1 ± 0.01, 2.6 ± 0.04, 4.6 ± 0.11, 3.78 ± 0.01, and 17.7 ± 0.03, 42.8 ± 0.06, 10.6 ± 0.13, 21.3 ± 0.03 µg/ml, respectively). This implying that the presence of monochloro and dichloro atoms of compounds **4a** and **4d**, respectively, on the phenyl ring at 4-position of the 4*H*-pyrano[3,2-*h*]quinoline was indispensable regarding the activities of the four cancer cells as compared to the other substituents and/or hetero moiety. Additionally, the IC₅₀ values of the second series **6a–h** decreased for the first members (monosubstituent, **6a**, IC₅₀ = 5.79 ± 0.01 and 3.01 ± 0.11 µg/ml) and the second members (disubstituent, **6d** IC₅₀ = 1.24 ± 0.3 and 1.83 ± 0.2 µg/ml) with respect to breast cancer and human hepatocellular carcinoma, while the values increased (moderate to weak activities) for the third and fourth members (polysubstituents and hetero group) in comparison to the standard drugs Vinblastine and Colchicine (IC₅₀ = 6.1 ± 0.01, 4.6 ± 0.11, and 17.7 ± 0.03, 10.6 ± 0.13 µg/ml, respectively), which suggests that the replacement of hydrogen atom with monochloro and dichloro atoms of compounds **6a** and **6d**, respectively, together with the methyl group at the 9-position was imperative for the activities against breast cancer and human hepatocellular carcinoma. Further investigation of the impact of the substitution patterns on the phenyl or hetero ring at the 4-position with the chloro atom at the 6-position of the 4*H*-pyrano[3,2-*h*]quinoline moiety has rendered the first members (monosubstituent, **8a, b** IC₅₀ = 0.9 ± 0.07, 3.04 ± 0.2, 0.7 ± 0.06, 2.67 ± 0.07 and 0.99 ± 0.01, 5.81 ± 0.11, 1.23 ± 0.03, 3.1 ± 0.01 µg/ml, respectively) and second members (disubstituent, **8d, e** IC₅₀ = 2.47 ± 0.13, 7.94 ± 0.05, 1.48 ± 0.11, 15.6 ± 0.13 and 1.18 ± 0.14, 3.01 ± 0.22, 0.87 ± 0.12, 1.79 ± 0.14 µg/ml, respectively) with a remarkable enhancement in their antitumor activities against the four tumor cell types, intimating that grafting lipophilic electron-withdrawing substituents like the halogens may be more advantageous than the other substituents and that the monosubstituent is more active than the disubstituent. Finally, we can deduce that the substitution patterns on the phenyl or hetero ring at the 4-position of the 4*H*-pyrano[3,2-*h*]quinoline moiety is a crucial element for the antitumor activity. The incorporation of electron-donating groups as the methyl group (hydrophobic group) at the 9-position is not favorable for activity while the substitution of bulky electron-withdrawing groups as the chlorine atom (hydrophobic group) at the 6-position has greatly enhanced the activity.

Conclusion

The biological study was executed to analyze the outcome of the substituents at different positions on the antitumor

behavior. Most of the targeted compounds exhibited good antitumor activities towards the evaluated tumor cell lines. Additionally, we found that these potent cytotoxic compounds induce cell cycle arrest at the G2/M phases and trigger apoptotic cell death for the four different cell lines. Furthermore, the SAR of the desired molecules highlighted the effect of the substituents at the 4-, 6-, and 9-positions on the antitumor activity.

Experimental section

Materials and equipments

All chemicals were purchased from Sigma-Aldrich Chemical Co. (Sigma-Aldrich Corp., St. Louis, MO, USA). All melting points measured with a Stuart Scientific Co. Ltd. apparatus are uncorrected. The IR spectra were recorded on a KBr disc on a Jasco FT/IR 460 plus spectrophotometer. The $^1\text{H}/^{13}\text{C}$ NMR (500/125 MHz) spectra were measured on BRUKER AV 500 MHz spectrometer in DMSO- d_6 as a solvent, using tetramethylsilane (TMS) as an internal standard, and chemical shifts (δ) are expressed in parts per million (ppm). The microwave apparatus used is Milestone Sr1, Microsynth. The mass spectra were determined on a Shimadzu GC/MS-QP5050A spectrometer. Elemental analysis was carried out at the Regional Centre for Mycology and Biotechnology (RCMP), Al-Azhar University, Cairo, Egypt, and the results were within $\pm 0.25\%$. Reaction courses and product mixtures were routinely monitored by TLC on silica gel-precoated F₂₅₄ Merck plates.

General procedure for synthesis of 2-amino-4-aryl-4H-pyrano[3,2-h]quinoline-3-carbonitrile derivatives (4a–h, 6a–h, 8a–i)

A reaction mixture of 8-hydroxyquinoline (**1**), 8-hydroxy-2-methylquinoline (**5**) or 5-chloro-8-hydroxyquinoline (**7**) (0.01 mol), with different aryl or hetaryl aldehydes (**2a–h**, or **2a–i**) (0.01 mol) and malononitrile (**3**) (0.01 mol) in ethanol catalyzed by piperidine under microwave irradiation conditions was heated for 2 min at 140 °C. After completion of the reaction, the reaction mixture was cooled to room temperature and the precipitated solid was filtered off, washed with methanol, and was recrystallized from ethanol or ethanol/benzene. The physical and spectral data of compounds **4a–h**, **6a–h** and **8a–i** are as follows.

2-Amino-4-(3-chlorophenyl)-4H-pyrano[3,2-h]quinoline-3-carbonitrile (4a)

Yellow crystals from ethanol; yield 84%; m.p. 241–242 °C (Lit. m.p. 240–241 °C; Fouda 2017).

2-Amino-4-(4-bromophenyl)-4H-pyrano[3,2-h]quinoline-3-carbonitrile (4b)

Yellow needles, yield 81%; m.p. 231–232 °C (Lit. m.p. 230–231 °C; El-Agrody and Al-Ghamdi 2011).

2-Amino-4-(2,6-difluorophenyl)-4H-pyrano[3,2-h]quinoline-3-carbonitrile (4c)

Yellow crystals from ethanol; yield 85%; m.p. 292–294 °C; IR (KBr, ν max cm^{-1}): 3481, 3330, 3219 (NH_2), 2190 (CN), 1663 (C=N); ^1H NMR (500 MHz, DMSO- d_6) δ : 8.95–7.06 (m, 8H, aromatic), 7.30 (bs, 2H, NH_2), 5.42 (s, 1H, H-4); ^{13}C NMR (125 MHz, DMSO- d_6) δ : 161.56 (C-2), 150.29 (C-9), 143.66 (C-10b), 137.23 (C-10a), 135.96 (C-7), 127.91 (C-5), 126.01 (C-6a), 123.70 (C-4a), 122.19 (C-8), 120.12 (C-6), 119.98 (CN), 52.78 (C-3), 30.56 (C-4), 160.80, 129.98, 119.73, 111.96 (aromatic); MS (m/z) with a base peak at 335 (M^+ , 100); $\text{C}_{19}\text{H}_{11}\text{F}_2\text{N}_3\text{O}$ (335.31); calcd; % C: 68.06, % H: 3.31, % N: 12.53; found; % C: 67.99, % H: 3.24, % N: 12.46.

2-Amino-4-(2,3-dichlorophenyl)-4H-pyrano[3,2-h]quinoline-3-carbonitrile (4d)

Yellow crystals from benzene; yield 85%; m.p. 280–281 °C (Lit. m.p. 240–241 °C; Fouda 2017).

2-Amino-4-(2,3,4,5,6-pentafluorophenyl)-4H-pyrano[3,2-h]quinoline-3-carbonitrile (4e)

Yellow crystals from benzene; yield 81%; m.p. 224–226 °C; IR (KBr, ν max cm^{-1}): 3412, 3338, 3186 (NH_2), 2194 (CN), 1661 (C=N); ^1H NMR (500 MHz, DMSO- d_6) δ : 8.96–7.21 (m, 5H, aromatic), 7.35 (bs, 2H, NH_2), 5.42 (s, 1H, H-4); ^{13}C NMR (125 MHz, DMSO- d_6) δ : 160.84 (C-2), 150.36 (C-9), 143.66 (C-10b), 136.00 (C-10a), 130.28 (C-7), 128.07 (C-5), 127.41 (C-6a), 123.85 (C-4a), 122.31 (C-8), 121.74 (C-6), 119.92 (CN), 52.36 (C-3), 31.01 (C-4), 142.63, 140.68, 137.21, 117.64 (aromatic); MS (m/z), 389 (M^+ , 30.38) with a base peak at 350 (100); $\text{C}_{19}\text{H}_8\text{F}_5\text{N}_3\text{O}$ (389.28); calcd; % C: 61.98, H, 3.01; N, 11.41; Found; % C: 61.95, % H: 2.99, % N: 11.39.

2-Amino-4-(thiophen-2-yl)-4H-pyrano[3,2-h]quinoline-3-carbonitrile (4f)

Yellow crystals from benzene; yield 81%; m.p. 261–262 °C; IR (KBr, ν max cm^{-1}): 3447, 3328, 3211 (NH_2), 2212 (CN), 1626 (C=N); ^1H NMR (500 MHz, DMSO- d_6) δ : 8.97–7.17 (m, 8H, aromatic and thiophene), 7.56 (s, 1H, thiophene H-5), 7.46 (bs, 2H, NH_2), 7.18 (s, 1H, thiophene H-3), 7.37 (bs, 2H, NH_2), 5.39 (s, 1H, H-4); ^{13}C NMR (125 MHz, DMSO- d_6) δ :

160.67 (C-2), 152.33 (C-9), 150.37 (C-10b), 137.39 (C-10a), 136.02 (C-7), 127.98 (C-5), 126.86 (C-6a), 123.97 (C-4a), 122.38 (C-8), 120.86 (C-6), 120.02 (CN), 55.22 (C-3), 36.30 (C-4), 142.57, 126.57, 123.37 (thiophene); MS (m/z), 305 (M^+ , 30.38) with a base peak at 222 (100); calcd; For $C_{17}H_{11}N_3OS$ (305.35); % C: 66.87, % H: 3.63, N, 13.76; Found; % C: 66.95, % H: 3.69, % N: 13.83.

2-Amino-4-(4-bromothiophen-2-yl)-4H-pyrano[3,2-*h*]quinoline-3-carbonitrile (4g)

Yellow crystals from benzene; yield 80%; m.p. 258–260 °C; IR (KBr, ν max cm^{-1}): 3387, 3317, 3193 (NH_2), 2202 (CN), 1661 (C=N); 1H NMR (500 MHz, DMSO- d_6) δ : 8.96–7.43 (m, 5H, aromatic), 7.55 (s, 1H, thiophene H-5), 7.37 (bs, 2H, NH_2), 7.18 (s, 1H, thiophene H-3), 5.38 (s, 1H, H-4); ^{13}C NMR (125 MHz, DMSO- d_6) δ : 160.62 (C-2), 152.38 (C-9), 150.37 (C-10b), 137.39 (C-10a), 136.07 (C-7), 127.98 (C-5), 126.89 (C-6a), 123.90 (C-4a), 123.33 (C-8), 120.86 (C-6), 120.02 (CN), 55.23 (C-3), 36.30 (C-4), 142.74, 126.57, 122.36, 108.16 (thiophene); MS (m/z), 385 ($M^+ + 2$, 96.19), 383 (M^+ , 100); calcd; For $C_{17}H_{10}BrN_3OS$ (384.25); % C: 53.14, % H: 2.62, N, 10.94; Found; % C: 53.09, % H: 2.57, % N: 10.90.

2-Amino-4-(pyridin-3-yl)-4H-pyrano[3,2-*h*]quinoline-3-carbonitrile (4h)

Yellow crystals from benzene; yield 80%; m.p. 264–265 °C; IR (KBr, ν max cm^{-1}): 3463, 3326, 3191 (NH_2), 2191 (CN), 1654 (C=N); 1H NMR (500 MHz, DMSO- d_6) δ : 8.48–7.20 (m, 9H, aromatic and pyridine), 7.31 (bs, 2H, NH_2), 5.08 (s, 1H, H-4); ^{13}C NMR (125 MHz, DMSO- d_6) δ : 160.44 (C-2), 150.31 (C-9), 148.76 (C-10b), 137.46 (C-10a), 136.00 (C-7), 127.83 (C-5), 126.89 (C-6a), 124.07 (C-4a), 122.26 (C-8), 120.92 (C-6), 120.192 (CN), 55.19 (C-3), 38.58 (C-4), 148.41, 143.22, 140.87, 135.42, 123.82 (pyridine); MS (m/z), 300 (M^+ , 32.82) with a base peak at 222 (100); calcd; For $C_{18}H_{12}N_4O$ (300.31); % C: 71.99, % H: 4.03, % N: 18.66. Found; % C: 71.93, % H: 3.98, % N: 18.60.

2-Amino-4-(3-chlorophenyl)-9-methyl-4H-pyrano[3,2-*h*]quinoline-3-carbonitrile (6a)

Yellow crystals from ethanol; yield 87%; m.p. 238–239 °C (Lit. m.p. 240–241 °C; Fouda 2017).

2-Amino-4-(4-bromophenyl)-9-methyl-4H-pyrano[3,2-*h*]quinoline-3-carbonitrile (6b)

Colorless needles, yield 75%; m.p. 279–280 °C (Lit. m.p. 230–231 °C; El-Agrody and Al-Ghamdi 2011).

2-Amino-4-(2,6-difluorophenyl)-9-methyl-4H-pyrano[3,2-*h*]quinoline-3-carbonitrile (6c)

Yellow crystals from ethanol; yield 81%; m.p. > 300 °C; IR (KBr, ν max cm^{-1}): 3454, 3341, 3223 (NH_2), 2194 (CN), 1655 (C=N); 1H NMR (500 MHz, DMSO- d_6) δ : 8.22–7.05 (m, 7H, aromatic), 7.17 (bs, 2H, NH_2), 5.40 (s, 1H, H-4), 2.71 (s, 3H, CH_3); ^{13}C NMR (125 MHz, DMSO- d_6) δ : 161.48 (C-2), 159.13 (C-9), 143.24 (C-10b), 136.23 (C-10a), 138.08 (C-7), 126.29 (C-5), 125.02 (C-6a), 123.53 (C-4a), 122.92 (C-8), 120.09 (C-6), 119.98 (CN), 52.88 (C-3), 30.60 (C-4), 24.97 (CH_3), 160.83, 129.95, 119.09, 111.96 (aromatic); MS (m/z), 349 (M^+ , 100); $C_{20}H_{13}F_2N_3O$ (349.33); calcd; % C: 68.76, % H: 3.75, % N: 12.03, found; % C: 68.70, % H: 3.71, % N: 11.96.

2-Amino-4-(3,4-dichlorophenyl)-9-methyl-4H-pyrano[3,2-*h*]quinoline-3-carbonitrile (6d)

Yellow crystals from benzene; yield 88%; m.p. 241–242 °C (Lit. m.p. 240–241 °C; Fouda 2017).

2-Amino-4-(2,3,4,5,6-pentafluorophenyl)-9-methyl-4H-pyrano[3,2-*h*]quinoline-3-carbonitrile (6e)

Yellow crystals from benzene; yield 80%; m.p. 295–296 °C; IR (KBr, ν max cm^{-1}): 3409, 3342, 3197 (NH_2), 2208 (CN), 1663 (C=N); 1H NMR (500 MHz, DMSO- d_6) δ : 8.24–7.12 (m, 4H, aromatic), 7.28 (bs, 2H, NH_2), 5.9 (s, 1H, H-4), 2.71 (s, 3H, CH_3); ^{13}C NMR (125 MHz, DMSO- d_6) δ : 160.87 (C-2), 159.21 (C-9), 143.22 (C-10b), 136.76 (C-10a), 130.15 (C-7), 126.63 (C-5), 125.09 (C-6a), 123.67 (C-4a), 123.03 (C-8), 119.96 (C-6), 118.32 (CN), 52.41 (C-3), 31.03 (C-4), 23.43 (CH_3), 142.50, 140.66, 136.09, 114.61 (aromatic); MS (m/z), 403 (M^+ , 96.79) with a base peak at 40 (100); $C_{20}H_{10}F_5N_3O$ (403.3); calcd; % C: 59.56, H, 2.50; N, 10.42. Found; % C: 59.46, % H: 2.41, % N: 10.38.

2-Amino-4-(thiophen-2-yl)-9-methyl-4H-pyrano[3,2-*h*]quinoline-3-carbonitrile (6f)

Yellow crystals from benzene; yield 84%; m.p. 268–269 °C; IR (KBr, ν max cm^{-1}): 3449, 3343, 3193 (NH_2), 2194 (CN), 1662 (C=N); 1H NMR (500 MHz, DMSO- d_6) δ : 9.08–7.22 (m, 4H, aromatic and thiophene), 7.57 (s, 1H, thiophene H-5), 7.43 (bs, 2H, NH_2), 7.33 (s, 1H, thiophene H-4), 7.22 (s, 1H, thiophene H-3), 5.35 (s, 1H, H-4), 2.71 (s, 3H, CH_3); ^{13}C NMR (125 MHz, DMSO- d_6) δ : 160.49 (C-2), 151.75 (C-9), 151.20 (C-10b), 138.08 (C-10a), 132.55 (C-7), 125.33 (C-5), 125.13 (C-6a), 123.49 (C-4a), 123.33 (C-8), 121.42 (C-6), 119.75 (CN), 55.14 (C-3), 36.04 (C-4), 23.42 (CH_3), 142.27, 127.18, 126.60 (thiophene); MS (m/z), 319 (M^+ , 38.38) with a base peak at 293 (100); calcd; For $C_{18}H_{13}N_3OS$ (319.38); %

C: 67.69, % H: 4.10, N, 13.16. Found; % C: 67.61, % H: 4.02, % N: 13.08.

2-Amino-4-(4-bromothiophen-2-yl)-9-methyl-4H-pyrano[3,2-*h*]quinoline-3-carbonitrile (6g)

Yellow crystals from benzene; yield 81%; m.p. 265–267 °C; IR (KBr, ν max cm^{-1}): 3465, 3329, 3198 (NH_2), 2190 (CN), 1652 (C=N); ^1H NMR (500 MHz, DMSO- d_6) δ : 9.05–7.65 (m, 4H, aromatic), 7.57 (s, 1H, thiophene H-5), 7.45 (bs, 2H, NH_2), 7.23 (s, 1H, thiophene H-3), 5.36 (s, 1H, H-4), 2.72 (s, 3H, CH_3); ^{13}C NMR (125 MHz, DMSO- d_6) δ : 160.43 (C-2), 151.76 (C-9), 151.20 (C-10b), 138.08 (C-10a), 132.52 (C-7), 126.19 (C-5), 125.36 (C-6a), 125.11 (C-4a), 123.49 (C-8), 121.42 (C-6), 119.75 (CN), 55.13 (C-3), 36.03 (C-4), 23.49 (CH_3), 142.21, 127.18, 123.60, 108.33 (thiophene); MS (m/z), 399 (M^+ +2, 5.95), 397 (M^+ , 6.05) with a base peak at 371 (100); calcd; For $\text{C}_{18}\text{H}_{12}\text{BrN}_3\text{OS}$ (398.28); % C: 54.28, % H: 3.04, N, 10.55. Found; % C: 54.36, % H: 3.11, % N: 10.60.

2-Amino-4-(pyridin-3-yl)-9-methyl-4H-pyrano[3,2-*h*]quinoline-3-carbonitrile (6h)

Yellow crystals from benzene; yield 82%; m.p. 281–282 °C; IR (KBr, ν max cm^{-1}): 3454, 3341, 3191 (NH_2), 2194 (CN), 1655 (C=N); ^1H NMR (500 MHz, DMSO- d_6) δ : 8.58–7.12 (m, 8H, aromatic and pyridine), 7.23 (bs, 2H, NH_2), 5.05 (s, 1H, H-4), 2.70 (s, 3H, CH_3); ^{13}C NMR (125 MHz, DMSO- d_6) δ : 160.48 (C-2), 159.11 (C-9), 148.80 (C-10b), 137.03 (C-10a), 136.08 (C-7), 126.32 (C-5), 125.66 (C-6a), 124.05 (C-4a), 122.93 (C-8), 120.93 (C-6), 120.21 (CN), 55.34 (C-3), 38.64 (C-4), 24.66 (CH_3), 148.37, 141.01, 135.35, 126.18, 123.81 (pyridine); MS (m/z), 314 (M^+ , 26.46) with a base peak at 236 (100); calcd; For $\text{C}_{19}\text{H}_{14}\text{N}_4\text{O}$ (314.34); % C: 72.60, % H: 4.49, % N: 17.82. Found; % C: 72.67, % H: 4.55, % N: 17.88.

2-Amino-6-chloro-4-(3-chlorophenyl)-4H-pyrano[3,2-*h*]quinoline-3-carbonitrile (8a)

Yellow crystals from benzene; yield 87%; m.p. 272–273 °C (Lit. m.p. 240–241 °C; Fouda 2017).

2-Amino-6-chloro-4-(4-bromophenyl)-4H-pyrano[3,2-*h*]quinoline-3-carbonitrile (8b)

Yellow crystals from ethanol; yield 88%; m.p. 229–230 °C (Lit. m.p. 240–241 °C; Fouda 2017).

2-Amino-6-chloro-4-(2,6-difluorophenyl)-4H-pyrano[3,2-*h*]quinoline-3-carbonitrile (8c)

Yellow crystals from ethanol; yield 82%; m.p. 298–290 °C; IR (KBr, ν max cm^{-1}): 3483, 3328, 3228 (NH_2), 2192 (CN), 1656 (C=N); ^1H NMR (500 MHz, DMSO- d_6) δ : 8.21–7.04 (m, 7H, aromatic), 7.18 (bs, 2H, NH_2 , D_2O exchangeable), 5.39 (s, 1H, H-4); ^{13}C NMR (125 MHz, DMSO- d_6) δ : 161.54 (C-2), 159.51 (C-9), 143.23 (C-10b), 136.07 (C-10a), 136.07 (C-7), 129.86 (C-5), 126.29 (C-6), 125.00 (C-6a), 123.52 (C-8), 120.10 (C-4a), 119.97 (CN), 52.88 (C-3), 30.59 (C-4), 160.83, 129.94, 119.85, 112.11 (aromatic); MS (m/z), 371 (M^+ , 30.62), 369 (M^+ , 100); $\text{C}_{19}\text{H}_{10}\text{ClF}_2\text{N}_3\text{O}$ (369.75); calcd; % C: 61.72, % H: 2.73, % N: 11.36; found; % C: 61.79, % H: 2.79, % N: 11.75.

2-Amino-6-chloro-4-(2,3-dichlorophenyl)-4H-pyrano[3,2-*h*]quinoline-3-carbonitrile (8d)

Pale yellow crystals from benzene; yield 87%; m.p. 300–301 °C (Lit. m.p. 240–241 °C; Fouda 2017).

2-Amino-6-chloro-4-(2,4-dichlorophenyl)-4H-pyrano[3,2-*h*]quinoline-3-carbonitrile (8e)

Pale yellow crystals from benzene; yield 85%; m.p. 276–277 °C (Lit. m.p. 240–241 °C; Fouda 2017).

2-Amino-6-chloro-4-(2,3,4,5,6-pentafluorophenyl)-4H-pyrano[3,2-*h*]quinoline-3-carbonitrile (8f)

Yellow crystals from benzene; yield 81%; m.p. 230–231 °C; IR (KBr, ν max cm^{-1}): 3404, 3335, 3189 (NH_2), 2195 (CN), 1660 (C=N); ^1H NMR (500 MHz, DMSO- d_6) δ : 9.07–7.44 (m, 4H, aromatic), 7.41 (bs, 2H, NH_2), 5.42 (s, 1H, H-4); ^{13}C NMR (125 MHz, DMSO- d_6) δ : 160.51 (C-2), 151.21 (C-9), 143.21 (C-10b), 137.83 (C-10a), 130.35 (C-7), 127.46 (C-5), 125.92 (C-6), 125.44 (C-6a), 123.49 (C-8), 122.93 (C-4a), 119.62 (CN), 52.41 (C-3), 30.75 (C-4), 142.63, 140.67, 132.44, 118.97 (aromatic); MS (m/z), 425 (M^+ +2, 18.15), 423 (M^+ , 5.91) with a base peak at 40 (100); $\text{C}_{19}\text{H}_7\text{ClF}_5\text{N}_3\text{O}$ (423.72); calcd; % C: 53.86, H, 1.67; N, 9.92. Found; % C: 53.80, % H: 1.61, % N: 9.86.

2-Amino-6-chloro-4-(thiophen-2-yl)-4H-pyrano[3,2-*h*]quinoline-3-carbonitrile (8g)

Yellow crystals from benzene; yield 80%; m.p. 283–282 °C; IR (KBr, ν max cm^{-1}): 3443, 3344, 3238 (NH_2), 2213 (CN), 1667 (C=N); ^1H NMR (500 MHz, DMSO- d_6) δ : 9.05–7.22 (m, 7H, aromatic and thiophene), 7.58 (s, 1H,

thiophene H-5), 7.48 (bs, 2H, NH₂), 7.24 (s, 1H, thiophene H-3), 7.47 (bs, 2H, NH₂), 5.38 (s, 1H, H-4); ¹³C NMR (125 MHz, DMSO-d₆) δ: 160.42 (C-2), 151.79 (C-9), 151.25 (C-10b), 138.06 (C-10a), 132.53 (C-7), 127.43 (C-5), 126.19 (C-6), 125.35 (C-6a), 123.60 (C-8), 121.43 (C-4a), 119.78 (CN), 55.06 (C-3), 35.98 (C-4), 142.23, 127.19, 125.38, 123.38 (thiophene); MS (m/z), 341 (M⁺+2, 32.08) with a base peak at 339 (M⁺, 100); calcd; For C₁₇H₁₀ClN₃OS (339.8); % C: 60.09, % H: 2.97, N, 12.37. Found; % C: 60.00, % H: 2.90, % N: 12.30.

2-Amino-6-chloro-4-(4-bromothiophen-2-yl)-4H-pyrano[3,2-h]quinoline-3-carbonitrile (8h)

Yellow crystals from benzene; yield 80%; m.p. 279–280 °C; IR (KBr, *v* max cm⁻¹): 3387, 3297, 3240 (NH₂), 2204 (CN), 1660 (C=N); ¹H NMR (500 MHz, DMSO-d₆) δ: 9.05–7.65 (m, 4H, aromatic), 7.58 (s, 1H, thiophene H-5), 7.48 (bs, 2H, NH₂), 7.23 (s, 1H, thiophene H-3), 5.37 (s, 1H, H-4); ¹³C NMR (125 MHz, DMSO-d₆) δ: 160.41 (C-2), 151.78 (C-9), 151.21 (C-10b), 138.06 (C-10a), 132.53 (C-7), 127.49 (C-5), 126.19 (C-6), 125.34 (C-6a), 123.61 (C-8), 121.41 (C-4a), 119.79 (CN), 55.05 (C-3), 35.99 (C-4), 142.18, 127.18, 123.50, 108.34 (thiophene); MS (m/z), 420 (M⁺+4, 20.08), 418 (M⁺+2, 99.08), 416 (M⁺, 59.41) with a base peak at 354 (100); calcd; For C₁₇H₉BrClN₃OS (418.69); % C: 48.77, % H: 2.17, N, 10.04. Found; % C: 48.85, % H: 2.24, % N: 10.11.

2-Amino-6-chloro-4-(pyridin-3-yl)-4H-pyrano[3,2-h]quinoline-3-carbonitrile (8i)

Yellow crystals from benzene; yield 80%; m.p. 273–274 °C; IR (KBr, *v* max cm⁻¹): 3358, 3328, 3192 (NH₂), 2190 (CN), 1660 (C=N); ¹H NMR (500 MHz, DMSO-d₆) δ: 9.02–7.36 (m, 8H, aromatic and pyridine), 7.35 (bs, 2H, NH₂), 5.07 (s, 1H, H-4); ¹³C NMR (125 MHz, DMSO-d₆) δ: 160.22 (C-2), 151.07 (C-9), 148.81 (C-10b), 138.11 (C-10a), 132.37 (C-7), 126.25 (C-5), 125.18 (C-6), 125.03 (C-6a), 123.31 (C-4a), 121.42 (C-8), 119.92 (CN), 55.10 (C-3), 38.36 (C-4), 148.61, 142.70, 140.36, 135.47, 124.13 (pyridine); MS (m/z), 336 (M⁺+2, 3.88) 334 (M⁺, 12.07) with a base peak at 112 (100); calcd; For C₁₈H₁₁ClN₄O (334.76); % C: 64.58, % H: 3.31, % N: 16.74. Found; % C: 64.51, % H: 3.24, % N: 16.67.

Biological screening

Cell culture

The tumor cell lines breast adenocarcinoma (MCF-7), human colon carcinoma (HCT-116), hepatocellular carcinoma (HepG-2) and lung carcinoma (A549) were obtained from the American Type Culture Collection (ATCC,

Rockville, MD). The cells were grown on RPMI-1640 medium supplemented with 10% inactivated fetal calf serum and 50 µg/ml gentamycin. The cells were maintained at 37 °C in a humidified atmosphere with 5% CO₂ and were subcultured 2–3 times a week.

Cytotoxicity evaluation using viability assay

The tumor cell lines were suspended in the medium at a concentration of 5 × 10⁴ cells/well in Corning® 96-well tissue culture plates and then incubated for 24 h. The tested compounds with concentrations ranging from 0 to 50 µg/ml were then added into 96-well plates (six replicates) to achieve different conc. for each compound. Six vehicle controls with media or 0.5% DMSO were run for each 96-well plate as a control. After incubating for 24 h, the numbers of viable cells were determined by the MTT test. Briefly, the media was removed from the 96-well plates and replaced with 100 µl of fresh culture RPMI-1640 medium without phenol red then 10 µl of the 12 mM MTT stock solution (5 mg of MTT in 1 ml of PBS) to each well including the untreated controls. The 96-well plates were then incubated at 37 °C and 5% CO₂ for 4 h. An 85-µl aliquot of the media was removed from the wells, and 50 µl of DMSO was added to each well and mixed thoroughly with the pipette and incubated at 37 °C for 10 min. Then, the optical density was measured at 590 nm with the microplate reader (Sunrise, TECAN, Inc, USA) to determine the number of viable cells and the percentage of viability was calculated as [1 – (ODt/ODc)] × 100%, where ODt is the mean optical density of wells treated with the tested sample and ODc is the mean optical density of untreated cells. The relation between surviving cells and drug concentration is plotted to get the survival curve of each tumor cell line after treatment with the specified compound. The 50% inhibitory concentration (IC₅₀), the concentration required to cause toxic effects in 50% of intact cells, was estimated from graphic plots of the dose–response curve for each conc. (Demirci and Bas,er 2002; Rahman et al. 2001; Mosmann 1983).

Cell cycle analysis

Cell cycle analysis was carried out using a Propidium Iodide Flow Cytometry Kit (Abcam, UK) (Qu et al. 2016; Shen et al. 2009). Different cell lines were seeded in a six-well plate at a concentration of 5 × 10⁴ per well, then incubated for 24 h. Cells were cultured for an additional 24 h in the absence (control) or presence of tested newly synthesized compounds with a concentration equal to the IC₅₀ value. After that cells were harvested and fixed using 66% ethanol on ice, and stored at 4 °C for at least 2 h. After rewashing with PBS, cells were resuspended in 200 µl of 1 × propidium iodide + RNase staining solution for 30 min at room temperature in the dark. The DNA content in each cell

nucleus was determined by a FACS Calibur flow cytometer (BD Biosciences, Franklin Lakes, NJ, USA). Finally, cell cycle phase distribution was analyzed using Cell Quest Pro software (BD Biosciences) showing collected propidium iodide fluorescence intensity on FL2.

Quantification of apoptosis by flow cytometry

Annexin V-FITC apoptosis assay was performed by using Annexin V-FITC/PI double staining detection kit (BD Pharmingen, USA) (Van Engeland et al. 1998; Vermes et al. 1995). Briefly, cells were cultured at a density of 5×10^4 per well in six-well plates, and treated with IC₅₀ concentration of the different tested compounds for 24 h. The staining procedure was performed following the manufacturer's instruction. Flow cytometric analysis was performed on FACS Calibur flow cytometer (BD Biosciences, Franklin Lakes, NJ, USA). Annexin V-FITC was detected through (FL1) channel, while PI was detected through the (FL2) channel. Finally, a minimum of 10,000 cells per sample were acquired and analyzed using Cell Quest Pro software (BD Biosciences).

Statistics

All data were expressed as the means \pm standard deviation (SD), from at least three independent experiments with similar results. Statistical analysis and figures were performed by GraphPad Prism 5.01 (GraphPad software, San Diego, CA, USA).

Acknowledgements The authors extend their appreciation to the Deanship of Science Research at King Khalid University for funding this work through General Research Project under Grant Number (G. R.P-168-39). In addition, the authors deeply thank the Regional Center for Mycology & Biotechnology (RCMP), Al-Azhar University, Cairo, Egypt, for carrying out the antitumor study and also, Mr. Ali Y. A. Alshahrani for drawing the ¹H NMR and ¹³C NMR spectra.

Compliance with ethical standards

Conflict of interest The authors declare that they have no conflict of interest.

Publisher's note: Springer Nature remains neutral with regard to jurisdictional claims in published maps and institutional affiliations.

References

- Al-Ghamdi AM, Abd EL-Wahab AHF, Mohamed HM, El-Agrody AM (2012) Synthesis and antitumor activities of 4*H*-pyrano[3,2-*h*]quinoline-3-carbonitrile, 7*H*-pyrimido[4',5':6,5]pyrano[3,2-*h*]quinoline, and 14*H*-Pyrimido[4',5':6,5]pyrano[3,2-*h*][1,2,4]triazolo[1,5-*c*]quinoline derivative. *Lett Drug Des Discov* 9:459–470
- Balamurugan K, Jeyachandran V, Perumal S, Manjashetty TH, Yogeewari P, Sriram D (2010) A microwave-assisted, facile, regioselective Friedländer synthesis and antitubercular evaluation of 2,9-diaryl-2,3-dihydrothieno[3,2-*b*]quinolones. *Eur J Med Chem* 45:682–688
- Batt DG, Petraitis JJ, Sherk SR, Copeland RA, Dowling RL, Taylor TL, Jones EA, Magolda RL, Jafee BD (1998) Heteroatom- and carbon-linked biphenyl analogs of Brequinar as immunosuppressive agents. *Bioorg Med Chem Lett* 8:1745–1750
- Cairns H, Cox D, Gould K, Ingall A, Suschitzky J (1985) New anti-allergic pyrano[3,2-*g*]quinoline-2, 8-dicarboxylic acids with potential for the topical treatment of asthma. *J Med Chem* 28:1832–1834
- Chang FS, Chen W, Wang C, Tzeng CC, Chen YL (2010) Synthesis and antiproliferative evaluations of certain 2-phenylvinylquinoline (2-styrylquinoline) and 2-furanylvinylquinoline derivatives. *Bioorg Med Chem* 18:124–133
- Chen IS, Tsai IL, Teng C, Chen JJ, Chang YA, Ko FN, Lu MC, Pezzuto JM (1997) Pyranoquinoline alkaloids from *Zanthoxylum simulans*. *Phytochemistry* 46:525–529
- Chen IS, Wu SJ, Tsai IL, Wu TS, Pezzuto JM, Lu MC, Chai H, Suh N, Teng CMJ (1994) Chemical and bioactive constituents from *Zanthoxylum simulans*. *Nat Prod* 57:1206–1211
- Chen J, Chen P, Liao C, Huang S, Chen I (2007) New phenylpropenoids, bis (1-phenylethyl) phenols, bisquinolinone alkaloid, and anti-inflammatory constituents from *Zanthoxylum integrifolium*. *J Nat Prod* 70:1444–1448
- Demirci F, Bas,er KHC (2002) Bioassay techniques for drug development By Atta-ur-Rahman, M. Iqbal Choudhary (HEJRIC, University of Karachi, Pakistan), William J. Thomsen (Areana Pharmaceuticals, San Diego, CA). Harwood Academic Publishers, Amsterdam, the Netherlands. xii+223pp. *J Nat Prod* 65:1086–1087
- Doube D, Blouin M, Brideau C, Chan C, Desmarais C, Ethier D, Falgueyret JP, Friesen RW, Girard M, Girard Y, Guay J, Tagari P, Young RN (1998) Quinolines as potent 5-lipoxygenase inhibitors: synthesis and biological profile of L-746,530. *Bioorg Med Chem Lett* 8:1255–1260
- Edmont D, Rocher R, Plisson C, Chenault J (2000) Synthesis and evaluation of quinoline carboxyguanidines as antidiabetic agents. *Bioorg Med Chem Lett* 10:1831–1834
- El-Agrody AM, Abd-Rabboh HSM, Al-Ghamdi AM (2013) Synthesis, antitumor activity, and structure-activity relationship of some 4*H*-pyrano[3,2-*h*]quinolone and 7*H*-pyrimido[4',5':6,5]pyrano[3,2-*h*]quinolone derivatives. *Med Chem Res* 22:1339–1355
- El-Agrody AM, Al-Ghamdi AM (2011) Synthesis of certain novel 4*H*-pyrano[3,2-*h*]quinoline derivatives ARKIVOC xi_134–146
- El-Agrody AM, Khattab ESAEH, Fouda AM, Al-Ghamdi AM (2012) Synthesis and antitumor activities of certain novel 2-amino-9-(4-halostyryl)-4*H*-pyrano[3,2-*h*]quinoline derivatives. *Med Chem Res* 12:4200–4213
- Fouda AM (2017) Halogenated 2-amino-4*H*-pyrano[3,2-*h*]quinoline-3-carbonitriles as antitumor agents and structure-activity relationships of the 4-, 6-, and 9-positions. *Med Chem Res* 26:302–313
- Hammouda MAA, EL-Hag FA-AA, El-Serwy WS, El-Manawaty MA (2015) Synthesis and characterization of new fused 4*H*-Pyranoquinoline carbonitrile derivatives with anticipated antitumor biological activity. *RJPBCS* 6:200–208
- Hassanin HM, Ibrahim MA, Alnamer YA-S (2012) Synthesis and antimicrobial activity of some novel 4-hydroxyquinolin-2(1*H*)-ones and pyrano[3,2-*c*]quinolinones from 3-(1-ethyl-4-hydroxy-2-oxo-1,2-dihydroquinolin-3-yl)-3-oxopropanoic acid. *Turk J Chem* 36:682–699
- Isaka M, Tanticharoen M, Kongsaeere P, Thebtaranonth Y (2001) Structures of cordypyridones A–D, antimalarial *N*-hydroxy- and *N*-methoxy-2-pyridones from the insect pathogenic fungus *Cordyceps nipponica*. *J Org Chem* 66:4803–4808

- Kamperdick C, Van NH, Van Sung T, Adam GB (1999) Bisquinolinone alkaloids from *Melicope ptelefolia*. *Phytochemistry* 50:177–181
- Kappe CO (2004) Controlled microwave heating in modern organic synthesis. *Angew Chem Int Ed* 43:6250–6284
- Kaur K, Jain M, Kaur T, Jain R (2009) Antimalarials from nature. *Bioorg Med Chem* 17:3229–3256
- Kidwai M, Saxena S, Khan MKR, Thukra SS (2005) Aqua mediated synthesis of substituted 2-amino-4*H*-chromenes and in vitro study as antibacterial agents. *Bioorg Med Chem Lett* 15:4295–4298
- Koizumi F, Fukumitsu N, Zhao J, Chanklan R, Miyakawa T, Kawahara S, Iwamoto S, Suzuki M, Kakita S, Rahayu E, Hosokawa S, Tatsuta K (2007) YCM1008A, a novel Ca²⁺-signaling inhibitor, produced by *Fusarium* sp. YCM1008. *J Antibiot* 60:455–458
- Maalej E, Chabchoub F, Oset-Gasque MJ, Esquivias-Pérez M, González MP, Monjas L, Pérez C, de los Ríos C, Rodríguez-Franco MI, Iriepa I, Moraleda I, Chioua M, Romero A, Marco-Contelles J, Samadi A (2012) Synthesis, biological assessment, and molecular modeling of racemic 7-aryl-9,10,11,12-tetrahydro-7*H*-benzo[7,8]chromeno[2,3-*b*]quinolin-8-amines as potential drugs for the treatment of Alzheimer's disease. *Eur J Med Chem* 54:750–763
- Magesh CJ, Makesh SV, Perumal PT (2004) Highly diastereoselective inverse electron demand (IED) Diels–Alder reaction mediated by chiral salen–AlCl complex: the first, target-oriented synthesis of pyranoquinolines as potential antibacterial agents. *Bioorg Med Chem Lett* 14:2035–2040
- Marco JL, Martínez-Grau A (1997) Friedländer reaction on 2-amino-3-cyano-4*H*-pyrans: synthesis of derivatives of 4*H*-pyrano[2, 3-*b*]quinoline, new tacrine analogues. *Bioorg Med Chem Lett* 7:3165–3170
- Mekheimer RA, Sadek KU (2009) Microwave-assisted reactions: three-component process for the synthesis of 2-amino-2-chromenes under microwave heating *Chin Chem Lett* 20:271–274
- Mol W, Matyia M, Filip B, Wietrzyk J, Boryczka S (1984) Synthesis and antiproliferative activity in vitro of novel (2-butynyl) thioquinolines. *Bioorg Med Chem* 16:8136–8141
- Mosmann T (1983) Rapid colorimetric assay for cellular growth and survival: application to proliferation and cytotoxicity assays. *J Immunol Methods* 65:55–63
- Narsinh D, Anamik S (2001) Synthesis and anti-HIV studies of some substituted pyrimidinediones, ethoxy pyrano (3,2-*C*) quinolines and hydrazino pyrano (3,2-*C*) quinolines. *Ind J Pharm Sci* 63:211–215
- Nesterova IN, Alekseeva LM, Andreeva LM, Andreeva NI, Golovira SM, Granik VG (1995) Synthesis and study the pharmacological activity of derivatives of 5-dimethylaminopyrano-[3,2-*c*]quinolin-2-ones *Pharm Chem J* 29:111–114
- Prasad P, Shobhashana PG, Patel MP (2017) An efficient synthesis of 4*H*-pyranoquinolinone derivatives catalyzed by a versatile organocatalyst tetra-*n*-butylammonium fluoride and their pharmacological screening. *R Soc Open Sci* 4:170764. <https://doi.org/10.1098/rsos.170764>.
- Qu Z, Cui J, Harata-Lee Y, Aung TN, Feng Q, Raison JM (2016) Identification of candidate anti-cancer molecular mechanisms of Compound Kushen Injection using functional genomics. *Oncotarget* 10:66003–66019
- Rahman AU, Choudhary MI, Thomsen WJ (2001) *Bioassay technique for drug development*. Harwood Academic Publishers, Reading, UK.
- Ramesh M, Mohan PA, Shanmugam P (1984) A convenient synthesis of flindersine, atanine and their analogues. *Tetrahedron* 40:4041–4049
- Sechi M, Rizzi G, Bacchi A, Carcelli M, Rogolino D, Pala N, Sanchez TW, Taheri L, Dayam R, Neamati N (2009) Design and synthesis of novel dihydroquinoline-3-carboxylic acids as HIV-1 integrase inhibitors. *Bioorg Med Chem* 17:2925–2935
- Shen JK, Du HP, Yang M, Wang YG, Jin J (2009) Casticin induces leukemic cell death through apoptosis and mitotic catastrophe. *Ann Hematol* 88:743–752
- Shi A, Nguyen TA, Battina SK, Rana S, Takemoto DJ, Chiang PK, Hua DH (2008) Synthesis and anti-breast cancer activities of substituted quinolones. *Bioorg Med Chem Lett* 18:3364–3368
- Shi L, Wang M, Fan CA, Zhang FM, Tu YQ (2004) Microwave-promoted three-component coupling of aldehyde, alkyne, and amine via C–H activation catalyzed by copper in water. *Org Lett* 6:1001–1003
- Silveri S, Radhika T, Harinadha BV, Raj S, Madhava RB (2017) Synthesis and biological evaluation of pyrano[3,2-*h*]quinoline carbonitriles. *Int J Green Pharm* 11:S423–S429
- Sparatore A, Basilico N, Casagrande M, Parapini S, Taramelli D, Brun R, Wittlin S, Sparatore F (2008) Antimalarial activity of novel pyrrolizidinyl derivatives of 4-aminoquinoline. *Bioorg Med Chem Lett* 18:3737–3740
- Surpur MP, Kshirsagar S, Samant SD (2009) Exploitation of the catalytic efficacy of Mg/Al hydrotalcite for the rapid synthesis of 2-aminochromene derivatives via a multicomponent strategy in the presence of microwaves. *Tetrahedron Lett* 50:719–722
- Thomas KD, Adhikari AV, Shetty NS (2010) Design, synthesis and antimicrobial activities of some new quinoline derivatives carrying 1,2,3-triazole moiety. *Eur J Med Chem* 45:3803–3810
- Van Engeland M, Nieland LJW, Ramaekers FCS, Schutte B, Reutelingsperger CPM (1998) Annexin V-affinity assay: a review on an apoptosis detection system based on phosphatidylserine exposure. *Cytometry* 31:1–9
- Vermes I, Haanen C, Steffens-Nakken H, Teuteling C (1995) A novel assay for apoptosis: flow cytometric detection of phosphatidylserine expression on early apoptotic cells using fluorescein labeled annexin V. *J Immunol Methods* 184:39–51
- Wabo HK, Tane P, Connolly JD, Okunji CC, Schuster B, Iwu MM (2005) Tabouensinium chloride, a novel quaternary pyranoquinoline alkaloid from *Araliopsis tabouensis*. *Nat Prod Res* 19:591–595
- Wu X, Larhed M (2005) Microwave-enhanced aminocarbonylations in water. *Org Lett* 7:3327–3329